



GSICS Correction Algorithm for Geostationary Imagers

CGMS-36 recommended (36.11) **“the GSICS Executive Panel to consider establishing in 2009 an end-to-end demonstration toward an operational GSICS by including beta-users in the GSICS process.”** A comprehensive description of the GSICS operation, with sufficient details of theoretical basis for the design and generation of the products, is necessary to involve the users into the GSICS process. This paper is part of the effort to fill these needs.

GSICS Correction Algorithm for Geostationary Imagers

1 INTRODUCTION

This document describes the theoretical basis of the GSICS baseline algorithm that guides the inter-calibration between a radiometer on a GEO and a hyperspectral instrument on a LEO such as AIRS and IASI. The goal of this specific inter-calibration is to make the GEO radiances consistent with AIRS and IASI. Traceability of AIRS/IASI to internationally accepted standard such as SI, while desirable, is beyond the scope of this document. The algorithm has been designed in collaboration with GSICS partners and implemented at NOAA, JMA, EUMETSAT, KMA, and CMA.

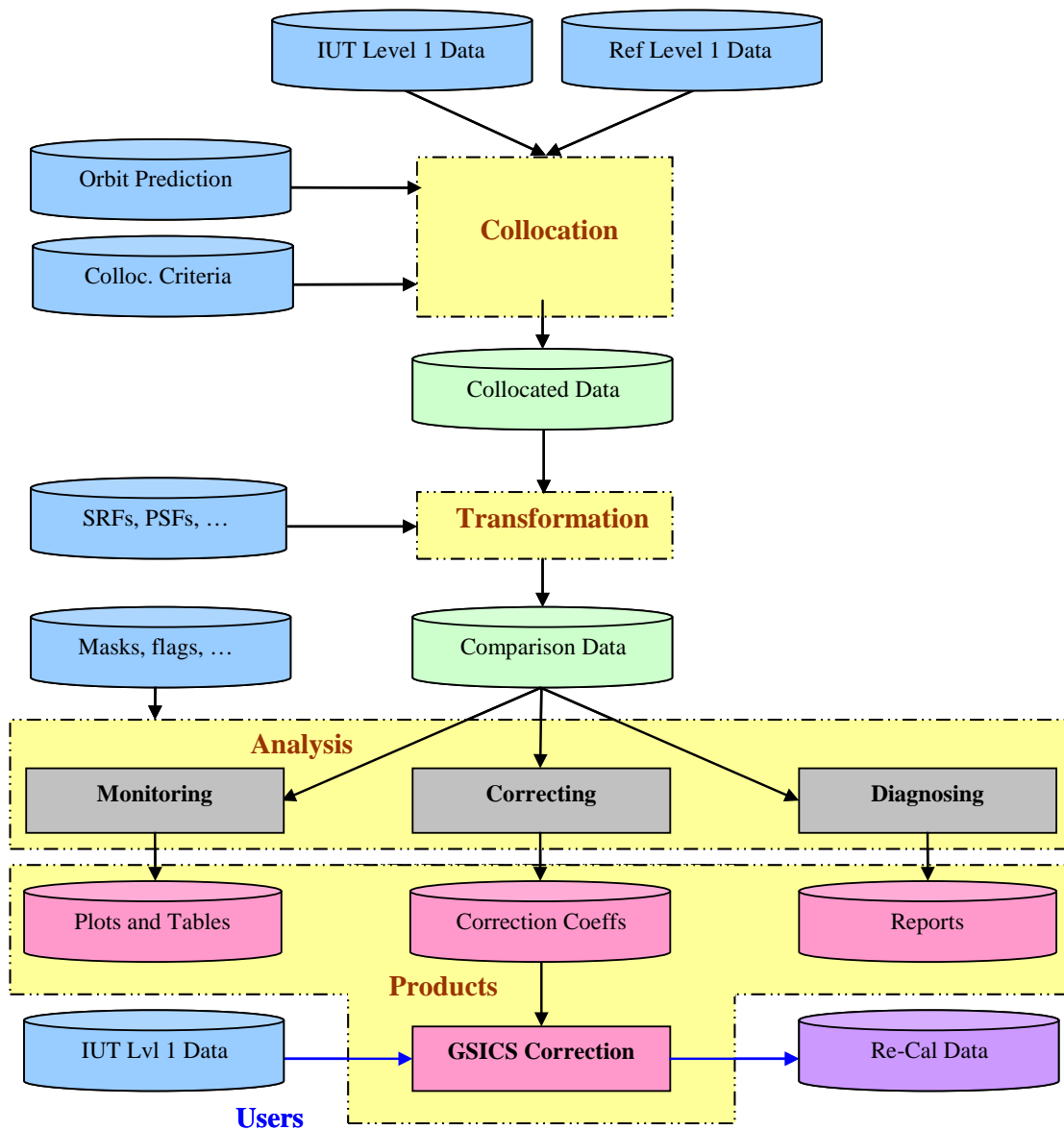


Figure 1: Flow chart of GSICS GEO-LEO Baseline Algorithm.

Inter-calibration is the systematic quantification of instrument responses to the signal inferred by a reference instrument, while both instruments are in normal operation. A prerequisite for inter-calibration is that two instruments view some common targets at the same time, with the same spatial and spectral responses, and the same viewing geometry. Since these idealized conditions rarely exist, in reality inter-calibration is a series of processes to subset, collocate, transform, select, and analyze the radiance by two instruments such that any and all such differences are minimized and/or otherwise properly accounted for, as illustrated in Fig. 1. The residual difference, if any, leads to GSICS Correction that homogenizes all the GEO observations to the common reference established by AIRS and IASI. A baseline algorithm is summarized here that are common to GEO-LEO inter-calibration in general. Algorithms for specific GEO-LEO pairs can be found at GSICS web site (<http://www.star.nesdis.noaa.gov/smcd/spb/calibration/icvs/GSICS/index.php>).

2. ALGORITHM

2.1 Principle of Data Collection

GSICS has three broad objectives. The first objective is to quantify the bias, or the difference between a GEO and AIRS/IASI, *for the collocated data*. This is useful because the results are generalized, albeit often implicitly, to measurements by the same pair of satellites *not* being directly compared. The second objective is to correct for the bias, again the efficacy of correction can only be validated with the collocated data but is assumed to hold for all measurements. The third objective is to find the cause of bias, thus to eliminate them from the root.

For all these objectives, it is important to evaluate the bias, correction, and cause analysis collectively or separately under a variety of conditions. This dictates that the collocated measurements should adequately cover the normal range of several aspects of data acquisition. Firstly, the collocations should cover all spectral bands, which enables user to quantify possible spectral variation of bias.

Secondly, the collocations should cover all scene temperatures, which enables user to quantify possible scene dependence of bias. For this reason, it is desirable to reduce the size of collocation, to single pixel if possible. Collocations over large area have other advantages, for example they are less sensitive to target non-uniformity and temporal non-concurrency, however they tend to smooth out scene temperature variability.

Next, the collocations should cover all ranges of geographic location, viewing geometry, and time of day, which enable user to quantify possible geographic, geometric (angular), and diurnal variation of bias. They all require that the collocations include those away from the GEO nadir. Note that both AIRS and IASI are on a sun-synchronous orbit (Aqua and METOP-A, respectively), which means they always pass the nadir of a geostationary satellite at the fixed local time of day.

Finally, the collocations should cover all days of year and all stage of satellite age, which enable user to quantify possible seasonal variation and long term trend of bias. They require that GSICS be operated continuously throughout the life time of satellites. In summary, *GSICS objectives require that single pixel collocations anywhere within the GEO field of regard be collected continuously over long term for all bands.*

As mentioned before, few collocations will be perfect; they are considered “collocated” if within certain threshold. Another principle for GSICS algorithm is therefore to set the threshold values reasonably tight to keep the data volume manageable, meanwhile sufficiently tolerant to allow down selection later by different users for various applications.

2.2 Subsetting

Only a minority amount of LEO granules are within a GEO’s field of regard (FOR), and only a small portion of which are concurrent with GEO. Also, a LEO granule collocated with a GEO image in time and space covers only a small portion of the GEO image. As a result, only a small subset of both GEO and LEO data, typically 2-5%, is possible to generate collocations. It helps to identify this small subset of data to greatly improve the efficiency of the algorithm.

The GEO FOR is defined in this context as any locations whose arc angle (angular distance) to GEO nadir is less than a threshold or, equivalently, the cosine of this angle is larger than a threshold. Assuming the earth is spherical and the earth coordinates of GEO nadir G (0, geo_nad_lon) and granule center P (gra_ctr_lat , gra_ctr_lon) are known, the arc angle between GEO nadir and granule center can be computed with cosine theorem for a right angle on a sphere (see Fig. 2):

Equation 1:
$$\cos(GP) = \cos(gra_ctr_lat)\cos(geo_nad_lon - gra_ctr_lon)$$

The maximum scan angle for both IASI and AIRS is $\sim 50^\circ$. Considering the mean orbit height for Aqua (705 km) and METOP-A (817 km), the maximum zenith angle for all AIRA/IASI pixels is $\sim 60^\circ$. Because of the requirement for similar GEO and LEO zenith angle, there is no need for GEO pixel with zenith angle much more than 60° , or pixels that are much more than 52° from the GEO nadir. So the threshold is $\cos(GP) > 0.6$. Note that $\cos(53^\circ) \approx 0.6$.

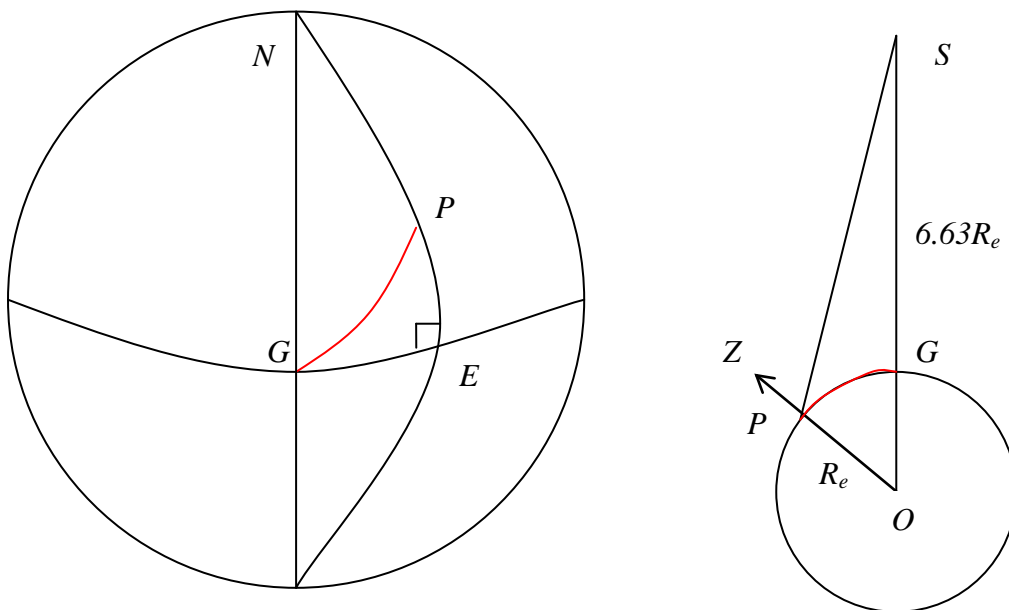


Figure 2: Computation of arc angle to satellite nadir and zenith angle of satellite from an earth location.

After a LEO granule is confirmed to be within a GEO's FOR, it is subject to verification that the granule is concurrent with GEO image. The threshold for concurrency may depend in part on the refresh rate of the GEO. For SEVIRI onboard METEOSAT-8/9 that typically refreshes every 15 minutes, a threshold of 7.5 minutes nearly guarantees that any LEO granule will collocate with a SEVIRI image. An even larger threshold could enable one LEO granule to be collocated with more than one SEVIRI images, which can be beneficial as long as one can handle the increasing amount of somehow duplicated data. On the other hand, for FY-2X that typically refreshes every hour, a threshold value of 7.5 minutes may result in very few collocations. This is because that, compared to the LEO's apparent movement in the FOR, FY-2X scans so slow that only a small portion of its image is concurrent with the LEO unless the threshold is loosened. A default value of half of GEO's refresh rate is recommended.

2.3 Collocation

A pair of GEO and LEO measurements is collocated in space when the GEO pixel closest to the LEO pixel is found through operational navigation. They are concurrent in time when the LEO pixel time and GEO scan line time are within the specified time window. Finally, they are aligned in line-of-sight when the difference between their zenith angle and azimuth angle is small.

The requirement for similar zenith angle means similar geometric path length, which implies similar optical path length if the optical property of the atmosphere is locally isotropic. A commonly used threshold is to limit the difference between the zenith angles of GEO and LEO to, say, less than 1°. For the purpose of achieving similar path length, which is proportional to the secant of zenith angle, this criterion tends to be more restrictive near the nadir. An alternative threshold is to limit the difference between the secant of the zenith angles of GEO and LEO. This criterion, on the other hand, tends to be more restrictive away from the nadir.

A compromise is to evaluate the relative difference of GEO and LEO path length with $|\cos(\text{geo_zen})/\cos(\text{leo_zen})-1|$. The threshold for this metric can be quite large for window channels (e.g., 0.05 for 10.7 μm channel) but must be rather small for more absorptive channels (e.g., <0.02 for 13.3 μm channel). A threshold value 0.01 is recommended for all channels.

In addition, relative azimuth angle of GEO and LEO line-of-sight is important for channels with reflective component. Since this is not an issue for longwave IR channels, no collocation is discarded solely due to azimuth angle, however the azimuth angles of GEO and LEO are included in the dossier for each collocation.

These angles are computed for GEO with the aid of Fig. 2. After computing the arc angle GP with Eq. 1, one applies the cosine theorem to an arbitrary triangle on a plane (the right panel of Fig. 2):

Equation 2:
$$SP^2 = SO^2 + OP^2 - 2 * SO * OP \cos(PG)$$

The zenith angle is computed with the sine theorem:

Equation 3: $\sin(SPZ) = \sin(PG) * SO / SP$

Similarly, one applies the sine theorem of spherical trigonometry to the arbitrary triangle GPN (the right panel of Fig. 2):

Equation 4: $\sin(GPN) = \sin(geo_nad_lon - gra_ctr_lon) / \sin(GP)$

since $\sin(NG) = 1$. The azimuth angle $[-\pi, \pi]$ is defined as the angle rotated clockwise from true north to the satellite line-of-sight projected on the earth surface or, more precisely, the plane tangent on the earth surface at the pixel, as illustrated in Fig. 3.

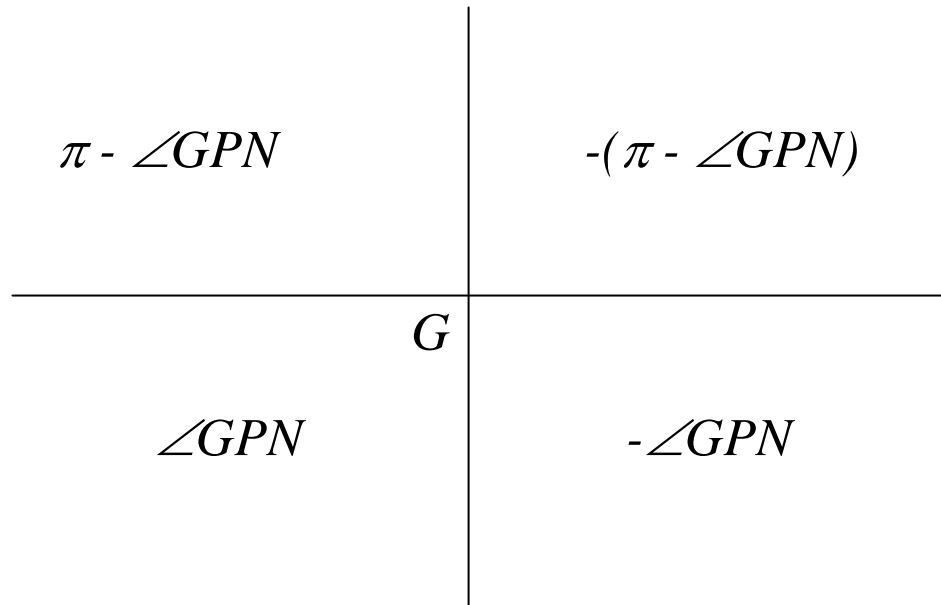


Figure 3: Computation of azimuth angle.

2.4 Transformation

The instantaneous field of view (FOV), spatial response such as point spread function, and spectral response function (SRF) of two instruments being compared are not necessarily identical. These differences should be accounted for before the two instruments can be compared.

2.4.1 FIELD OF VIEW

The FOV of imagers on GEO is smaller than that of the sounder on LEO (Fig. 4). After the GEO pixel (i, j) closest to the center of LEO pixel is identified, radiance from the neighboring 3-by-3 GEO pixels, $R_{ii,jj}^{GEO}$, are averaged to compute R_{Col}^{GEO} , the GEO radiance at the collocation:

Equation 5:
$$R_{Col}^{GEO} = \frac{1}{9} \sum_{ii=i-1}^{i+1} \sum_{jj=j-1}^{j+1} R_{ii,jj}^{GEO}$$

Non-uniform spatial response of GEO and LEO within its respective FOV is ignored. Some GEOs (e.g., GOES) over-sample along scan line, which call for special treatment.

2.4.2 ENVIRONMENT

The R_{Col}^{GEO} computed from Eq. 5 can mismatch the true LEO FOV in several ways. As illustrated in Fig. 4, there may be gaps between GEO FOVs; the actual LEO FOV may be larger or smaller than 3-by-3 GOE FOVs; and the navigation of either satellite can be uncertain that the FOVs are not exactly where they are supposed to be. The largest source of error, however, is often because the non-concurrency of GEO and LEO measurements. For example, if GOE images the LEO FOV a few minutes later and the mean movement of features in the area is as indicated in Fig. 4, the GEO would measure something different at the same place but later time or, effectively, another location at the same time.

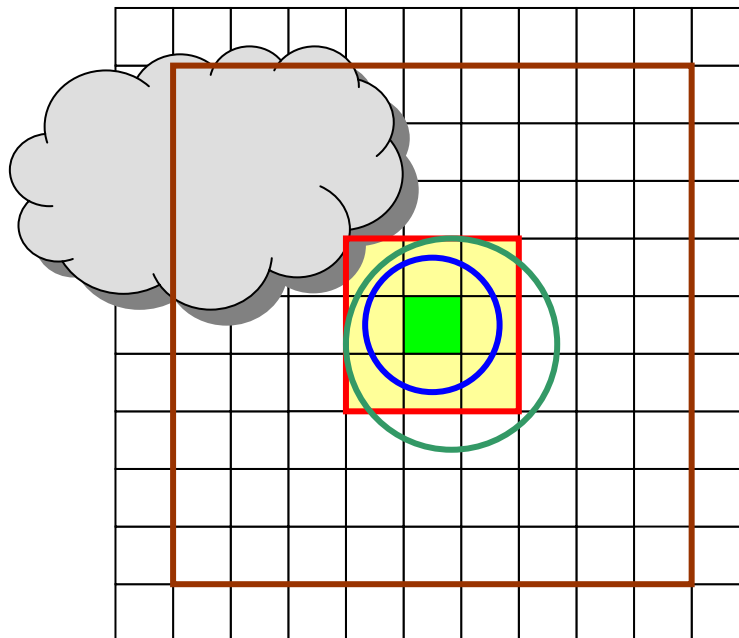


Figure 4: Illustration of spatial consideration in inter-calibration. The small circles represent GEO FOV. The shaded is the one closest to the center of LEO FOV, which is typically 3-by-3 of the size of GEO FOV but can be slightly smaller or larger. The small box of 3-by-3 GEO FOVs and the big box of 9-by-9 GEO FOVs are intercalibration “FOV” and “environment”, respectively. See text for more details.

To properly account for this discrepancy, it is noted that if the “environment” of the collocation is uniform, then one needs to concerns none of the issues mentioned above. Therefore the uniformity of the environment, represented by the standard deviation of the GEO measurements, should be computed now and considered later in analysis. The size of the environment should be defined according to the time window and the expected speed of feature movement, e.g., mean wind speed. Based on empirical studies, it is recommended to be 9-by-9 pixels for time window of about 10 minutes.

2.4.3 SPECTRAL CONVOLUTION

Omitting fine structures of LEO spectral response, the LEO radiance at the collocation, R_{Col}^{LEO} , can be simulated from R_{ν}^{LEO} , the LEO spectral radiance at wavenumber ν , and Φ_{ν}^{GEO} , the GEO spectral response at wavenumber ν :

Equation 6:

$$R_{Col}^{LEO} = \frac{\int_{\nu} R_{\nu}^{LEO} \Phi_{\nu}^{GEO} d\nu}{\int_{\nu} \Phi_{\nu}^{GEO} d\nu}$$

One issue, which is particularly acute for AIRS, is to estimate the R_{ν} that is not available, either due to design (spectral gaps or shortage) or operation (dead or unstable detectors). Tahara and Kato^[10] estimate these radiances as a linear combination of radiances available from other hyperspectral channels. The coefficients of the linear combination (or weights) are estimated from simulations of eight atmospheric profiles representative of the expected measurement conditions.

The R_{Col}^{GEO} and R_{Col}^{LEO} form the core of collocation. These, together with LEO spectral radiances R_{ν}^{LEO} , GEO spatial radiances $R_{ii,jj}^{GEO}$, relevant statistics, and ancillary and auxiliary data, are saved as collocated data (ref. Fig. 1) for further comparison, analysis, or re-processing.

2.5 Selection

There can be many reasons users want to filter the collocated measurements in their analyses. One is to select certain conditions, for example day or night, clear or cloudy, nadir or off-nadir, and so on. There are endless ways to analyze the collocations for special interest of the user, and the algorithm has been designed for that need. Another reason is to narrow down the window of threshold. As mentioned in 2.1, one of the principles in acquiring collocated data is to collect more than the necessary (to the extent that the data volume remains manageable) for users to down select for various applications. Finally, data can be selected to avoid certain conditions that are believed to compromise or complicate the analysis, for example those collocations too close to sun-glint, or those with nearly 180° relative azimuth angle when analyzing the 3.9 μm channel data during daytime.

Note that it may appear tempting to select uniform scene and environment to alleviate the effect that GEO and LEO are not necessarily viewing the same target (ref. 2.4). This is equivalent to assigning a binary weight of 0 or 1 to the collocations, according to some subjectively determined threshold. Study showed that a superior approach is to assign the weight objectively, e.g., according to the standard deviation of the collocation environment.

Other than providing the flexibility and making a few recommendations, the algorithm does not enforce any selection nor generating any intermediate data or products from selection. For this reason, selection can be regarded as part of analysis.

2.6 Analysis

2.6.1 BIAS

The first objective of GSICS is to quantify the bias, or the difference between a GEO and AIRS/IASI in this case. The bias can be quantified in many ways, for example the (weighted)

mean difference between GEO and LEO radiances. If bias is dependent on scene radiance, which is often the case, the mean GEO-LEO difference will depend on the samples and therefore is not an accurate measurement of bias.

The recommended approach is to perform a weighted linear regression of collocated radiances from the reference instrument x and target instrument y :

Equation 7: $\hat{y}(x) = a + bx$

To fit the observed data to the above model, the chi-square merit function is minimized to derive a and b :

Equation 8:
$$\chi^2(a, b) = \sum_{i=1}^N \left(\frac{y_i - a - bx_i}{\sigma_i} \right)^2$$

where the weight σ_i is defined as

Equation 9:
$$\sigma_i^2 = s_i^2 + \delta_{LEO}^2 + \delta_{GEO}^2$$

where s_i is the standard deviation of the environment for the i^{th} collocation and δ_{LEO}^2 and δ_{GEO}^2 are LEO and GEO instrument radiometric noises (net equivalent delta-radiance, or NEdN). In most cases, s_i is the dominant component of σ_i , however Eq. 9 recognizes that instruments are not necessarily perfect. Also, the inclusion of instrument radiometric noise ensures that uniform targets with zero standard deviation do not lead to infinite weight. Eq. 8 can be solved with well established method^[11] that computes not only the coefficients a and b but also their uncertainty σ_a and σ_b and covariance for further analysis:

Equation 10:
$$a = \frac{\sum_{i=1}^N \frac{x_i^2}{\sigma_i^2} \sum_{i=1}^N \frac{y_i}{\sigma_i^2} - \sum_{i=1}^N \frac{x_i}{\sigma_i^2} \sum_{i=1}^N \frac{x_i y_i}{\sigma_i^2}}{\sum_{i=1}^N \frac{1}{\sigma_i^2} \sum_{i=1}^N \frac{x_i^2}{\sigma_i^2} - \left(\sum_{i=1}^N \frac{x_i}{\sigma_i^2} \right)^2}$$

Equation 11:
$$b = \frac{\sum_{i=1}^N \frac{1}{\sigma_i^2} \sum_{i=1}^N \frac{x_i y_i}{\sigma_i^2} - \sum_{i=1}^N \frac{x_i}{\sigma_i^2} \sum_{i=1}^N \frac{y_i}{\sigma_i^2}}{\sum_{i=1}^N \frac{1}{\sigma_i^2} \sum_{i=1}^N \frac{x_i^2}{\sigma_i^2} - \left(\sum_{i=1}^N \frac{x_i}{\sigma_i^2} \right)^2}$$

Equation 12:
$$\sigma_a^2 = \frac{\sum_{i=1}^N \frac{x_i^2}{\sigma_i^2}}{\sum_{i=1}^N \frac{1}{\sigma_i^2} \sum_{i=1}^N \frac{x_i^2}{\sigma_i^2} - \left(\sum_{i=1}^N \frac{x_i}{\sigma_i^2} \right)^2}$$

Equation 13:

$$\sigma_b^2 = \frac{\sum_{i=1}^N \frac{1}{\sigma_i^2}}{\sum_{i=1}^N \frac{1}{\sigma_i^2} \sum_{i=1}^N \frac{x_i^2}{\sigma_i^2} - \left(\sum_{i=1}^N \frac{x_i}{\sigma_i^2} \right)^2}$$

Equation 14:

$$\text{cov}(a, b) = \frac{-\sum_{i=1}^N \frac{x_i}{\sigma_i^2}}{\sum_{i=1}^N \frac{1}{\sigma_i^2} \sum_{i=1}^N \frac{x_i^2}{\sigma_i^2} - \left(\sum_{i=1}^N \frac{x_i}{\sigma_i^2} \right)^2}$$

In order to be directly comparable for representative scenes and conveniently expressed in units understandable by the users, bias are evaluated as the difference between a reference radiance x_{ref} and the regression estimate at that reference radiance. There are a number of ways to choose reference radiance, in fact it is possible to choose more than one reference radiances for various scenes. Current recommendation is to select the reference based on radiative transfer calculations, which has the advantage of being applicable to all GEOs. These are provided in Table 1.

Table 1: Reference radiance, expressed in terms of brightness temperature, for common GEO spectral channels.

Ch (μm)	3.9	6.2	7.3	8.7	9.7	10.8	12.0	13.4
T_{bstd} (K)	284	236	255	284	261	286	285	267

Mathematically, the bias is defined as:

Equation 15:

$$\Delta \hat{y}(x_{REF}) = a + bx_{REF} - x_{REF}$$

and the uncertainty of bias estimate is:

Equation 16:

$$\sigma_{\hat{y}}^2(x_{REF}) = \sigma_a^2 + \sigma_b^2 x_{REF}^2 + 2 \text{cov}(a, b) x_{REF}$$

The results may be expressed in absolute or percentage bias in radiance, or brightness temperature differences. An example of bias analysis is presented in Fig. 5.

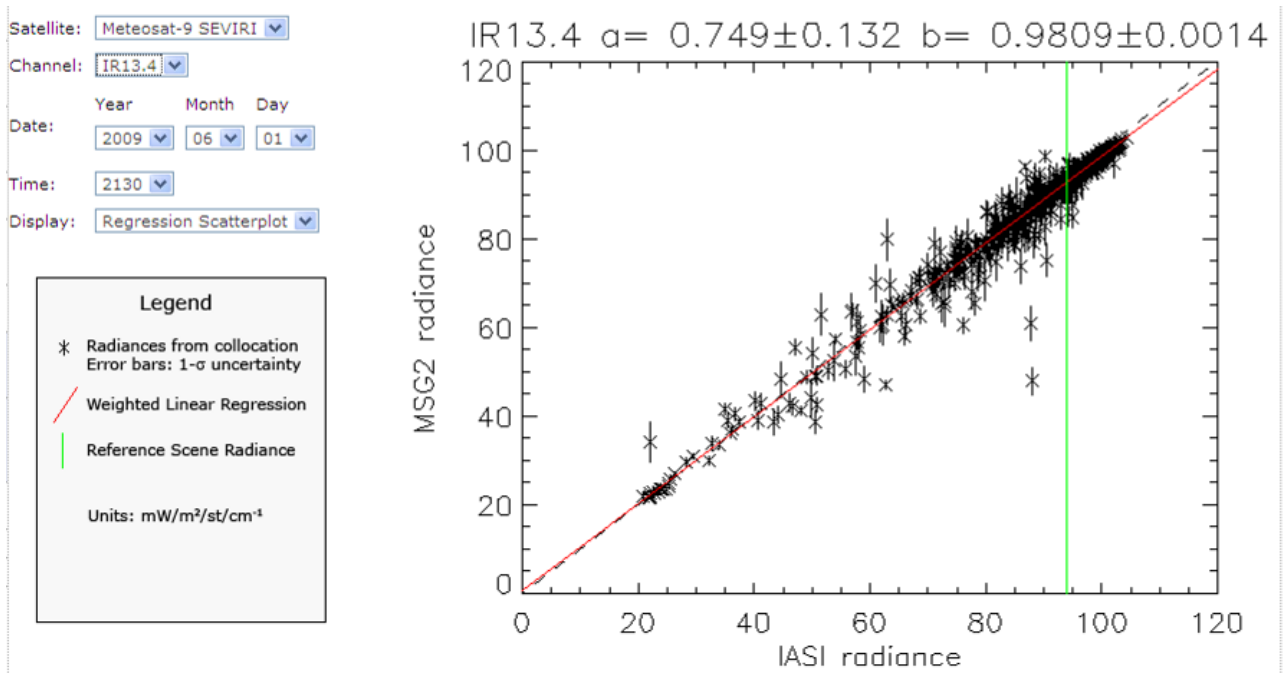


Figure 5: Scatter plot of comparison between IASI and SEVIRI on METEOSAT-9 for the 13.4 μm channel on June 1, 2009. The vertical bars associated with each symbol indicate collocation uncertainty, or standard deviation of collocation environment. The dashed diagonal line indicates where GEO and LEO radiances are identical. The **solid red line** is the result of linear regression. The **solid vertical green line** indicates the position of reference radiance. The difference between the red solid line and black dashed line at the position of the green vertical line is the bias, which is too small to be discerned in this plot.

2.6.2 CORRECTION

The second objective of GSICS is to correct for the bias. Since the bias is quantified in terms of regression (Eq. 7), the GSICS Correction is accordingly defined as

Equation 17:
$$R_{GSICS} = -\frac{a}{b} + \frac{1}{b} R_{GEO}$$

where R_{GEO} is the GEO radiance, a and b are the regression coefficients derived from Eqs. 10 & 11, and R_{GSICS} is GSICS corrected GEO radiance, which is consistent with AIRS and IASI.

One of the critical issues in defining GSICS Correction is the period of regression. In Eqs. 8 and 10-14, the choice of N , or the period of data collection, was not specifically defined. This is important because the GEO bias need to be allowed to vary slowly in unknown fashion, for example with certain seasonal variation and/or long term trend. The period therefore should be sufficiently short to catch this variation. On the other hand, the input data may be noisy such that, in short period, they may lead to large variation that is unrealistic for GEO instrument. Thus, the period of regression should be chosen to accommodate for both requirements.

Fig. 6 shows the impact of period of regression. The left panel shows the GSICS Correction based on regression over a 10 day period. The day-to-day variation of the correction has been

smaller than that using daily regression (not shown), however it still suggests that GOES calibration performance changes more rapidly than expected. When the period of regression is extended to 30 days (right panel), the results look reasonable. The period of regression is tentatively recommended to be 30 days, pending further revision.

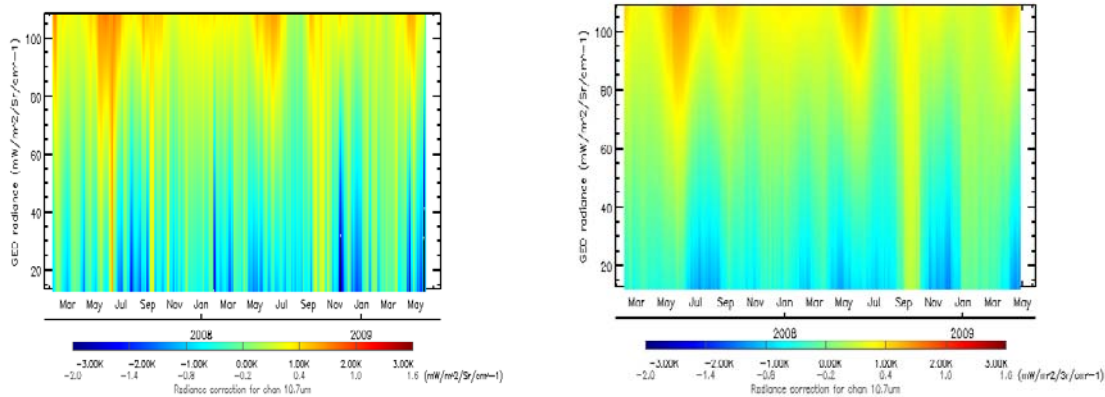


Figure 6: GSICS Correction, expressed in terms of brightness temperature, for GOES-11 10.7 μm channel over a two-year period and for various GEO radiances. The left panel shows the results for period of regression of 10 days; the right panel is the same but for 30 days.

Sometimes, GEO instrument performance may indeed have short term variation. An extreme example is the occasional instrument decontamination, which is known to change instrument performance. Another more common example is that GEO bias can vary diurnally, particularly those on 3-axis stabilized platforms. For these reasons only the similar data are used for regression, and periods marked by special event such as decontamination are analyzed separately.

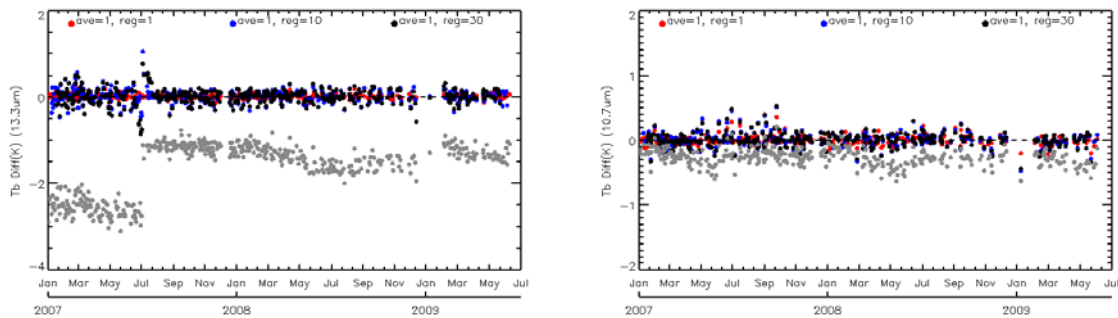


Figure 7: Time series of daytime mean biases for GOES-12 13.3 μm (left) and 10.7 μm channel (right) since beginning of 2007, compared to AIRS and expressed as brightness temperature, before (gray) and after (black) the GSICS Correction. Instrument decontaminations in February 2007, July 2007, and January 2009 created discontinuity in 13.3 μm channel bias. These and other time-dependent bias has been nearly eliminated. Large excursions of the GSICS corrected radiances associated with instrument decontaminations confirm the need to treat these periods separately. These periods, however, were deliberately combined to demonstrate that, had the decontamination not been known, the GSICS Correction would be able to identify them as instrument performance anomaly.

2.6.3 ROOT CAUSE ANALYSIS

The third objective of GSICS is to diagnose for the root cause of bias. There have been several successful examples for this type of applications, for example the diagnosis and correction of error in GOES-13 Imager 13.3 μm channel spectral response function^[12], and the characterization of GOES Imager midnight blackbody calibration anomaly^[13], which have been discussed elsewhere.

4. CONCLUSIONS

GSICS has an important mission of ensuring the comparability of satellite measurements provided at different times, using different instruments, and under the responsibility of different space agencies. The GEO-LEO intercalibration algorithm is an important step for GSICS to accomplish that mission. The algorithm has been carefully designed, through collaboration of international partners, to quantify, correct for, and diagnose the root cause of bias. Initial evaluation indicates that the algorithm performance is satisfactory. The next step is to invite users to test the products generated by the algorithm and to provide feedback for further improvements.

ACKNOWLEDGEMENTS

Many contributed to the development of the baseline algorithm, in particular the current and former members of GSICS Research Working Group, including D. Blumstein, C. Cao, S.-R. Chung, D. Doelling, M. Gunshor, P. Henry, T. Hewison (vice chair), X. Hu, D. Kim, M. König, J. Lafeuille, J. Liu, P. Minnis, A. Okuyama, J. Privette, B.-J. Sohn, Y. Tahara, D. Tobin, X. Xiong, L. Van de Berg, X. Wu (chair), P. Zhang, and Y. Zhang. F. Yu provided Figs. 6 & 7. The contents are solely the opinions of the authors and do not constitute a statement of policy, decision, or position on behalf of NOAA or the U. S. Government.

REFERENCES

- [1] Goldberg, M. D., 2007: Global space-based inter-calibration system (GSICS). *Atmospheric and Environmental Remote Sensing Data Processing and Utilization III: Readiness for GEOSS*, San Diego, CA, USA, SPIE, 668402-4.
- [2] Tobin, D. C.; Revercomb, H. E.; Knuteson, R. O.; Best, F. A.; Smith, W. L.; Ciganovich, N. N.; Dedecker, R. G., Dutcher, S., Ellington, S. D., Garcia, R. K., Howell, H. B., LaPorte, D. D., Mango, S. A., Pagano, T. S., Taylor, J. K., van Delst, P., Vinson, K. H. and Werner, M. W. (2006), Radiometric and spectral validation of Atmospheric Infrared Sounder observations with the aircraft-based Scanning High-Resolution Interferometer Sounder. *Journal of Geophysical Research*, 111, Doi:10.1029/2005JD006094, 2006.
- [3] Blumstein, D., B. Tournier, F. R. Cayla, T. Phulpin, R. Fjortoft, C. Buil, and G. Ponce, 2007: In-flight performance of the infrared atmospheric sounding interferometer (IASI) on METOP-A. *Atmospheric and Environmental Remote Sensing Data Processing and Utilization III: Readiness for GEOSS*, San Diego, CA, USA, SPIE, 66840H-12.
- [4] Aumann, H. H. and T. S. Pagano, 2008: Using AIRS and IASI data to evaluate absolute radiometric accuracy and stability for climate applications. *Atmospheric and Environmental Remote Sensing Data Processing and Utilization IV: Readiness for GEOSS II*, San Diego, CA, USA, SPIE, 708504-5.

- [5] Blumstein, D., E. Pequignot, B. Tournier, R. Fjortoft, L. Buffet, C. Larigauderie, T. Phulpin, and I. Gaudel, 2008: IASI FM2 on METOP A Performances after 1.5 year in orbit. *16th International TOVS Study Conferences*, Angra dos Reis, Brazil.
- [6] Strow, L., S. Hannon, D. Tobin, and H. Revercomb, 2008: Inter-Calibration of the AIRS and IASI operational infrared sensors. *17th annual CALCON Technical Conference*, Logan, UT, USA.
- [7] Tobin, D. C., H. Revercomb, F. Nagle, and R. Holz, 2008: Evaluation of IASI and AIRS spectral radiances using Simultaneous Nadir Overpasses. *16th International TOVS Study Conferences*, Angra dos Reis, Brazil.
- [8] Wang, L., X. Wu, Y. Li, M. Goldberg, S.-H. Sohn, and C. Cao, 2009: Comparison of AIRS and IASI Radiances Using GOES Imagers as Transfer Radiometers towards Climate Data Records. *Submitted to J. Appl. Meteor. Climate*.
- [9] Cao, C., M. Weinreb, and H. Xu, 2004, Predicting simultaneous nadir overpasses among polar-orbiting meteorological satellites for the intersatellite calibration of radiometers. *J. Atmos. Ocean. Tech.*, **21**, 537-542.
- [10] Tahara, Y. and K. Kato, 2008: New Spectral Compensation Method for Intercalibration with High Spectral Resolution Sounder. *Meteorological Satellite Center Technical Note*, **No. 52**.
- [11] Press, W. H., S. A. Teukolsky, W. T. Vetterling, and Brian P. Flannery, 1996: "Numerical Recipes in Fortran 90" (Section 15.2).
- [12] Wu, X., T. Schmit, R. Galvin, M. Gunshor, T. Hewison, M. König, Y. Tahara, D. Blumstein, Y. Li, S. Sohn, and m. Goldberg, 2008: Investigation of GOES Imager 13.3 μm channel cold bias. EUMETSAT Conference on Meteorological Satellite, Damstadt, Germany, September 8-12, 2008.
- [13] M. K. Rama Varma Raja, X. Wu, and F. Yu: Assessment of Midnight Blackbody Calibration Correction (MBCC) Using the Global Space-based Inter-Calibration System (GSICS), *Proc. SPIE 7456* (2009)